

**NEUTRON TOTAL CROSS SECTIONS OF ^{235}U FROM
TRANSMISSION MEASUREMENTS IN THE ENERGY
RANGE 2 keV to 300 keV AND STATISTICAL MODEL
ANALYSIS OF THE DATA**

**H. Derrien ,J. A. Harvey, N. M. Larson
L. C. Leal, and R. Q. Wright**

May 2000

Computational Physics and Engineering Division

**NEUTRON TOTAL CROSS SECTIONS OF ^{235}U
FROM TRANSMISSION MEASUREMENTS
IN THE ENERGY RANGE 2 keV to 300 keV
AND STATISTICAL MODEL ANALYSIS OF THE DATA**

H. Derrien
J. A. Harvey
N. M. Larson
L. C. Leal
R. Q. Wright

Date Published: April 2000

Prepared by the
OAK RIDGE NATIONAL LABORATORY
managed by
UT-BATTELLE, LLC
for the
U.S. DEPARTMENT OF ENERGY
under contract DE-AC05-00OR22725

CONTENTS

ACKNOWLEDGMENTS	<u>vii</u>
ABSTRACT	<u>1</u>
1. INTRODUCTION	<u>2</u>
2. EVALUATION OF THE AVERAGE TOTAL CROSS SECTION	<u>2</u>
2.1 GENERALITIES ON TRANSMISSIONS AND TOTAL CROSS SECTIONS	<u>2</u>
2.2 THE EXPERIMENTAL DATA	<u>4</u>
2.3 THE SELF-SHIELDING CORRECTION	<u>5</u>
2.4 THE AVERAGE TOTAL CROSS SECTION	<u>8</u>
3. STATISTICAL MODEL ANALYSIS OF THE EXPERIMENTAL DATA	<u>22</u>
3.1 THE SAMMY/FITACS STATISTICAL MODEL CODE	<u>23</u>
3.2 THE SAMMY/FITACS FIT OF THE AVERAGE CROSS SECTION	<u>23</u>
4. CONCLUSION	<u>30</u>
REFERENCES	<u>31</u>

LIST OF TABLES

Table 1. Calculated average effective cross sections and average true total cross sections in the energy range up to 20 keV. The data obtained from the resonance parameters of Ref. 3 are given in the first part of the table ($E < 2.2$ keV). Those obtained from a simulated sample of resonance parameters are given in the second part of the table ($E > 2.2$ keV).	<u>5</u>
Table 2. Average total cross section in the energy range 2 keV to 300 keV corrected for isotopic composition of the sample and for self-shielding effects	<u>8</u>
Table 3. Comparison between the experimental cross section of Poenitz et al. ⁴ with the present results averaged over the energy resolution of Poenitz.	<u>20</u>
Table 4. The parameters used as input in the SAMMY/FITACS calculations	<u>24</u>
Table 5. Parameters obtained from the SAMMY/FITACS fit of the experimental cross section in the energy range 2 keV to 200 keV.	<u>27</u>
Table 6. The renormalization coefficients as obtained from the SAMMY/FITACS fit of the experimental data	<u>28</u>

LIST OF FIGURES

<u>Figure</u>	<u>Page</u>
Figure 1. The self-shielding correction in the energy range up to 20 keV in the experimental conditions of the thick sample transmission of Harvey et al. ¹	7
Figure 2. Average total cross section in the energy range from 20 keV to 300 keV: present results (+), Uttley ⁸ data (x) and Poenitz ⁴ data (o).	21
Figure 3. Average total cross section in the energy range 40 keV to 300 keV: present results (+) and Poenitz ⁴ data (o).	21
Figure 4. Average total cross section in the energy range 2 keV and 300 keV: present results (+) and ENDF/B-VI data (o).	22
Figure 5. Experimental and calculated α values. The solid line represents an eye-guided fit of the experimental data. The short-dashed line represents the capture to fission ratio calculated at the output of the SAMMY/FITACS fit. The long-dashed line represents the values calculated from the ENDF/B-VI fission and capture cross sections. Experimental data: Δ de Saussure et al. ¹⁶ \diamond Corvi ¹³ \circ Weston et al. ²⁷ \times Muradyan et al. ¹⁴ $+$ Beer et al. ¹⁵ $*$ Perez et al. ²⁸	26
Figure 6. Average total cross sections in the energy range 2 keV to 200 keV: present results (+) and Poenitz results (o). The solid lines represent the results of the SAMMY/FITACS fit.	28
Figure 7. Average fission cross sections in the energy range 2 keV to 200 keV. The solid lines represent the results of the SAMMY/FITACS fit. Experimental data: \circ Blons ²² Δ Migneco et al. ²³ $+$ Wagemans et al. ²⁴ \times Weston et al. ²⁶ \diamond Perez et al. ²⁸	29
Figure 8. ENDF/B-VI fission (circles) and capture cross sections (crosses) compared to the results of the SAMMY/FITACS fit (solid line).	29
Figure 9. Average capture cross section. The solid lines represent the results of the SAMMY/FITACS fit. The circles represent the cross sections calculated by multiplying Weston fission data by the evaluated values of α . The structures are the results of the structures in Weston fission data and in the evaluated α data (the solid line in Fig.5).	30

ACKNOWLEDGMENTS

This work was sponsored by the U.S. Department of Energy (DOE), under contract DE-AC05-00OR22725 with Ut-Battelle, LLC. The authors are particularly indebted to D. Cabrilla, Office of Nuclear Facility Management, and H. Johnson, Environmental Management, U.S. Department of Energy, Washington, D.C., for their support.

ABSTRACT

The average ^{235}U neutron total cross sections were obtained in the energy range 2 keV to 330 keV from high-resolution transmission measurements of a 0.033 atom/b sample.¹ The experimental data were corrected for the contribution of isotope impurities and for resonance self-shielding effects in the sample. The results are in very good agreement with the experimental data of Poenitz et al.⁴ in the energy range 40 keV to 330 keV and are the only available accurate experimental data in the energy range 2 keV to 40 keV. ENDF/B-VI evaluated data are 1.7% larger. The SAMMY/FITACS code² was used for a statistical model analysis of the total cross section, selected fission cross sections and α data in the energy range 2 keV to 200 keV. SAMMY/FITACS is an extended version of SAMMY which allows consistent analysis of the experimental data in the resolved and unresolved resonance region. The Reich-Moore resonance parameters were obtained³ from a SAMMY Bayesian fits of high resolution experimental neutron transmission and partial cross section data below 2.25 keV, and the corresponding average parameters and covariance data were used in the present work as input for the statistical model analysis of the high energy range of the experimental data. The result of the analysis shows that the average resonance parameters obtained from the analysis of the unresolved resonance region are consistent with those obtained in the resolved energy region. Another important result is that ENDF/B-VI capture cross section could be too small by more than 10% in the energy range 10 keV to 200 keV.

1. INTRODUCTION

High resolution neutron transmission measurements of ^{235}U were performed by Harvey et al.¹ in the neutron energy range 0.5 eV to 300 keV using the Oak Ridge Electron Linear Accelerator (ORELA) as a pulsed neutron source. The experimental data were analyzed in the energy range 0.5 eV to 2.25 keV with the Reich-Moore Bayesian code SAMMY,² along with experimental fission and capture cross sections, in order to obtain the resonance parameters.³ The results of the analysis were included in ENDF/B-VI release 5. The average resonance parameters were also obtained from statistical analysis of the resonance spacings and the partial reaction widths.³ These average parameters could be used for a reevaluation of the cross sections in the unresolved energy range with the aim of matching the resolved-energy range with the unresolved-energy range at 2.25 keV. Statistical model or optical model codes are used for the calculation of the average cross sections in the unresolved-resonance range from the average resonance parameters and for comparison with average experimental cross sections; accurate average total cross sections are indispensable for a consistent evaluation of the partial cross sections. Unfortunately, the ^{235}U experimental total cross sections are scarce and not reliable in the energy range up to 50 keV, especially in a region where accurate values of the self-shielding factors are needed. Accurate values of the experimental average total cross sections could be obtained from Harvey et al. transmission measurements up to the neutron energy of about 300 keV.

The purpose of the present paper is to report on: (1) the evaluation of the experimental average total cross section from Harvey et al. thick sample transmission data in the energy range 2 keV to 300 keV, with the correction for the experimental effects, and (2) the analysis of the experimental average total cross section along with experimental fission, capture, and alpha data by using the statistical model code SAMMY/FITACS.² The results will be used as a basis for the reevaluation of ^{235}U cross sections in the unresolved range for ENDF/B-VI.

2. EVALUATION OF THE AVERAGE TOTAL CROSS SECTION

2.1 GENERALITIES ON TRANSMISSIONS AND TOTAL CROSS SECTIONS

The total neutron cross section $\sigma(E)$, at neutron energy E , is obtained from the neutron transmission $Tr(E)$ of a sample of thickness n by the relation:

$$Tr(E) = \exp(-n\sigma(E)) \quad (1)$$

where the cross section $\sigma(E)$ is given in barn(b) and n in atom/barn. However, the transmission of neutrons through the sample cannot be measured at the precise energy E of the neutrons, but is a value averaged over the experimental resolution in an energy interval $E1$ to $E2$ depending on the width of the resolution function. The quantity which is really measured is

$$Tr(\mathbf{E}) = \int_{E1}^{E2} \mathbf{exp}(-n\sigma_{\Delta}(\mathbf{E}')) R(\mathbf{E}-\mathbf{E}') d\mathbf{E}' , \quad (2)$$

where R is the experimental resolution function and $\sigma_{\Delta}(\mathbf{E}')$ is the Doppler broadened cross section at energy \mathbf{E}' .

Via the inversion of Eq. (1), one obtains the so-called average effective total cross section $\sigma_{eff}(\mathbf{E})$, instead of the true average total cross section $\sigma(\mathbf{E})$,

$$\sigma_{eff}(\mathbf{E}) = -\frac{1}{n} \ln(Tr(\mathbf{E})) . \quad (3)$$

It can be shown that $\sigma_{eff}(\mathbf{E})$ is smaller than the true average total cross section $\sigma(\mathbf{E})$. The difference between the average effective cross section and the true average cross section is due to the resonance structure of the data; it is the resonance self-shielding effect in the transmission measurement. This effect should be evaluated when deriving total cross section from transmission measurements. However, it can be neglected if $n\sigma(\mathbf{E})$ remains small in the energy interval $E1$ to $E2$, in such a way that $\mathbf{exp}(-n\sigma(\mathbf{E}))$ is very close to $1 - n\sigma(\mathbf{E})$ for all values of \mathbf{E} in the energy interval. This condition could be achieved by using thin samples in the transmission measurements. However, the experimental error on the effective cross section of thin samples is large since $d\sigma = (-1/n) dTr/Tr$, and could reach values much larger than the expected correction. For instance, the measurement of an effective total cross section of 20 barns with 1% accuracy needs a sample thickness of at least 0.05 atom/barn if the transmission is measured with 1% accuracy; the corresponding $n\sigma$ value is 1 and the self-shielding effect could still be quite large. It can be shown that the difference between the effective cross section and the true average total cross section depends, to first order, on the variance of the cross section, i.e., on the fluctuations of the cross section, over the energy width of the resolution function. Due to the resonance overlapping and possibly to the opening of new reaction channels, the fluctuations are decreasing when the neutron energy is increasing. Above an energy depending on the properties of the target nucleus, the fluctuations are small and the correction negligible even in thick samples.

When inferring average total cross section from transmission measurements three neutron energy ranges should be considered:

(a) The resolved energy range from thermal energy to an energy which depends on the average spacing of the resonances. In this energy range, high-resolution measurements allow the separation of almost all the large resonances, the width of the experimental resolution being smaller than the width of the resonances. The measured cross section varies from several barns between the resonances to several hundreds, or thousands, of barns in the peak of some resonances. The experimental data are usually analyzed in order to obtain the resonance parameters by using least-square or Bayesian fitting codes with proper nuclear reaction formalisms and taking into account the experimental effects of the transmission measurements. The values of the Doppler-broadened cross sections can then be recalculated from the resonance parameters by using the same formalism used in the analysis of the experimental data, giving the cross section free of the experimental effects. The self-shielding correction calculation is not needed in this method of data processing. However, the self-shielding corrections for cross sections averaged over several resonances can

be easily obtained by comparing calculated, or experimental, effective cross section, with calculated true average cross section. These “calculated” self-shielding corrections could be useful to check the variation with energy of the correction for a given experiment and sample, variation which could be extrapolated into the unresolved resonance range.

(b) The unresolved-resonance region, where the fluctuations of the measured cross section are due to unresolved multiplets of resonances, or to intermediate structure, which could hardly be analyzed in terms of single resonance parameters. The self-shielding corrections could be large and should be evaluated with good accuracy in order to obtain reliable values of the total cross section.

(c) The higher-energy range where the Doppler-broadened resonances overlap so much that there are no strong fluctuations in the cross section. The variation of the cross section is small over the energy range of the experimental resolution. The difference between the effective cross section and the true cross section is negligible. No correction is needed in this energy range.

The separation between the resolved- and unresolved-energy range is made by the analysts of the experimental data, who choose the upper energy limit beyond which realistic resonance analysis of the data could not be performed. In the case of ^{235}U data, the resonance analysis of the experimental data was performed up to 2.25 keV neutron energy. Therefore it is possible to evaluate the self-shielding corrections from data calculated with the resonance parameters in energy range up to 2.25 keV. Above this energy, the simulation of cross sections from resonance parameters obtained by Monte-Carlo sampling, or directly from the sample of parameters of the energy range 0 to 2.25 keV, should be used.

2.2 THE EXPERIMENTAL DATA

Detailed description of Harvey et al. transmission measurement of ^{235}U is found in Ref.1. The time-of-flight measurements were performed at an 80.4 m flight path for sample thicknesses of 0.0328 and 0.00236 atom/barn. The samples were cooled to liquid-nitrogen temperature in order to decrease the Doppler broadening of the resonances. The average total cross section of ^{235}U varies from about 20 b at 2 keV to about 9 b at 300 keV which corresponds to an average transmission of 0.52 and 0.74 respectively for the thick sample, and 0.95 and 0.97 respectively for the thin sample. An accuracy of 1% on the transmission measurement gave 0.3 b accuracy on the cross section measured from the thick sample and 4.3 b from the thin sample. Therefore only the thick sample was suitable for the evaluation of the average total cross section with a good accuracy. The thin sample measurement was used for the determination of the resonance parameters in the low energy range.³

The isotopic composition of the samples was 0.033% of ^{234}U , 0.184% of ^{236}U and 0.128% of ^{238}U . The samples also contained 0.385% of ^{181}Ta . The thickness of the samples increased by a factor of 1.006 in cooling to liquid-nitrogen temperature, giving a thickness of 0.03301 atom/barn of ^{235}U for the thick sample in the experimental conditions of the transmission measurements. Taking into account the isotopic analysis error and the error on the temperature correction, the error on the thickness was about 0.5%, i.e. 0.5% systematic error on the measured effective total cross section.

The normalization of the transmission ratio was obtained with 0.2% accuracy. The background correction was about 4% for the counting rate with the sample in the neutron beam and about 2% with the sample out of the beam. The background was measured with an accuracy of about 3%. Combining

quadratically these experimental errors, one obtains a systematic error of about 0.25% on the transmission ratio, corresponding to an absolute error of 0.08 b on the effective total cross section at all energies.

The contribution of ^{181}Ta and other U isotopes were calculated from ENDF/B-VI and subtracted point by point from the effective total cross section. As examples, the corrections at 2.2 keV, 13.5 keV and 326 keV were 0.13 b, 0.10 b and 0.06 b; i.e. 0.59%, 0.57% and 0.69% of the average total cross section, respectively. Assuming that the accuracy on the correction was about 10%, the corresponding error on the average effective total cross section was less than 0.1% at all energies.

2.3 THE SELF-SHIELDING CORRECTION

The resonance parameters in Ref.3 were obtained by fitting the transmission data of Harvey et al. with an accuracy better than 0.5% of the average transmission. The true average cross sections and the average effective cross sections could be calculated, with the same experimental conditions, from these parameters, for the evaluation of the corresponding self-shielding corrections. The results of the calculation performed with the code SAMMY are given in Table 1 in the energy range 0.2 keV to 2.2 keV for intervals of 0.2 keV (about 400 resonances in each energy interval). The difference between the calculated average true cross section and the calculated average effective cross section is the self-shielding effect at the experimental conditions of the transmission. As expected, the trend of the self-shielding effect is to decrease when the neutron energy increases, since the variation in the cross section decreases when the Doppler and experimental resolution widths increase. The strong fluctuations around the average correction were also expected, due in part to the Porter-Thomas fluctuations of the neutron widths.

Table 1. Calculated average effective cross sections and average true total cross sections in the energy range up to 20 keV. The data obtained from the resonance parameters of Ref. 3 are given in the first part of the table ($E < 2.2$ keV). Those obtained from a simulated sample of resonance parameters are given in the second part of the table ($E > 2.2$ keV).

Energy Range keV	Effective Total b	True Total b	Correction %
0.200-0.400	35.000	36.674	4.783
0.400-0.600	29.751	30.811	3.561
0.600-0.800	27.056	27.993	3.464
0.800-1.000	23.626	24.246	2.627
1.000-1.200	24.467	25.184	2.931
1.200-1.400	22.574	22.990	1.841
1.400-1.600	21.489	21.973	2.252
1.600-1.800	21.135	21.499	1.725

Table 1 (Contd.)

Energy Range keV	Effective Total b	True Total b	Correction %
1.800-2.000	20.993	21.605	2.915
2.000-2.200	19.700	20.025	1.649
-----	-----	-----	-----
2.200-2.400	20.295	20.680	1.897
3.200-3.400	19.075	19.352	1.452
4.200-4.400	17.981	18.182	1.118
5.200-5.400	17.277	17.434	0.909
6.200-6.400	16.936	17.062	0.744
8.200-8.400	16.583	16.679	0.579
10.200-10.400	15.795	15.859	0.405
15.200-15.400	15.215	15.252	0.243
20.200-20.400	14.266	14.290	0.168

In the unresolved range, above 2.25 keV neutron energy, the self-shielding correction can be evaluated by simulation of the data from resonance parameters obtained by Monte Carlo sampling using Wigner and Porter-Thomas distributions of spacings and widths, with average values inferred from the resolved resonance region, or obtained directly from the known set of resonance parameters shifted to the higher energy ranges. The second method was used in the present work, and contributions of p and d resonances were added. The calculation of the simulated data were performed with the code SAMMY in 9 energy interval of 200 eV in the energy range up to 20 keV. The results are given in the second part of Table 1. The corrections to the calculated average effective cross section have the same trend as in the resolved-resonance region, decreasing from about 2% to about 0.2%. The calculations were performed with an effective scattering radius of 9.60 fm obtained in the resonance analysis of the low energy region.³ This scattering radius gives the level of the smooth potential scattering cross section on which the resonance structures are seen. The resonance structures become small compared to the smooth scattering cross section when the neutron energy increases.

The values of the self-shielding correction versus energy are plotted in Fig.1 on a log-log scale. In this kind of representation, the behavior of the self-shielding correction is nearly linear in the energy range 2 keV to 20 keV. It is likely that the correction should be smaller than 0.1% in the energy ranges above 40 keV. Self-shielding corrections were also calculated by Poenitz et al.⁴ for effective total cross sections of a 0.097-atom/barn sample of ²³⁵U, a 0.06-atom/barn sample of ²³³U and a 0.089-atom/barn sample of ²³⁹Pu. They found that the correction was smaller than 1% above 50 keV for the isotopes considered. However, the correction for ²³⁵U should be much smaller than for ²³⁹Pu for comparable sample thickness, since ²³⁵U has average level spacing about four times smaller and also has more open channels; therefore a 1% correction could be a large overestimate for ²³⁵U in the Poenitz results. The thickness of the ²³⁵U sample used in Poenitz

experiments was three times larger than the one used by Harvey et al.; the calculations have shown that the self-shielding correction should be more than two times smaller for the Harvey sample. Another point of comparison with the results of Poenitz is found in Ref. 5 for ^{239}Pu , using the same method as in the present work; the correction was smaller than 1% at 50 keV, in agreement with the Poenitz conclusions for comparable sample thickness.

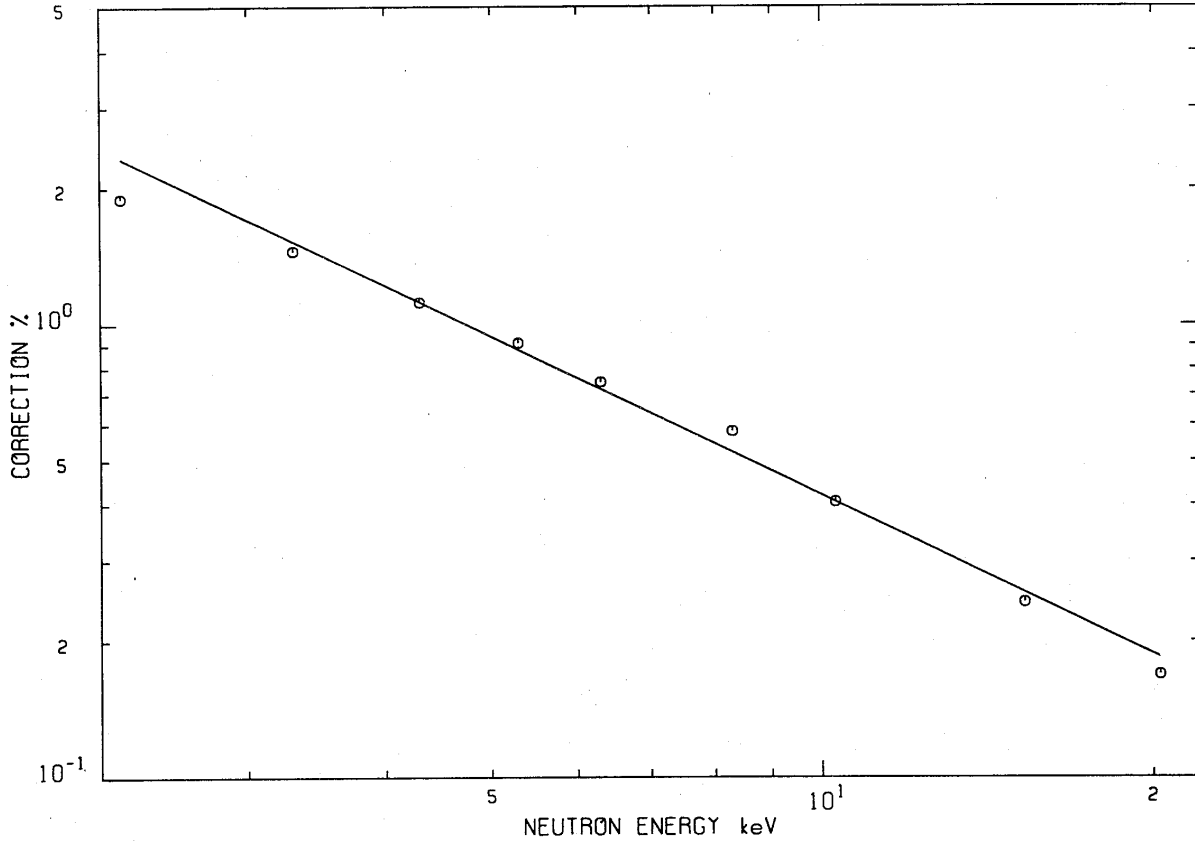


Figure 1. The self-shielding correction in the energy range up to 20 keV in the experimental conditions of the thick sample transmission of Harvey et al.¹

The linear trend of the variation of the self-shielding correction in Fig.1 can be represented by the following empirical relation in the energy range 2 keV to 20 keV:

$$k(E) = 0.0613 \exp(-1.165 \ln E) \quad (4)$$

where E is the energy in keV. The average true total cross section $\sigma(E)$ is then obtained by

$$\sigma(E) = (1 + k(E)) \sigma_{eff}(E) \quad (5)$$

2.4 THE AVERAGE TOTAL CROSS SECTION

The effective total cross section data of Harvey et al. obtained from the experimental transmission contains about 15,000 time-of-flight channel points in the energy range 2 keV to 326 keV. These data were corrected point by point for the contribution of other isotopes. The width of the resolution function was about 0.6 eV at 2 keV and about 0.8 keV at 300 keV. The average spacing of the s-wave resonances is about 0.45 eV. In the low energy region, the correction point-by-point of the data for the self-shielding effect is not possible by using the relation in Eq. (5) because the resolution function extends only on a small number of resonances. The energy interval used to calculate the simulated average data for the evaluation of the self-shielding effects shown on Table 1 was 0.2 keV and concerns about 400 s-wave resonances. The error induced on the true total cross section by applying the smooth correction of relation 5 is about 20% of the correction if the data are averaged over 200 eV energy range, i.e. 0.4%, 0.08%, 0.04% of the cross section, respectively, at 2 keV, 10 keV, 20 keV neutron energies.

Table 2 shows the values of the true total cross section averaged in energy intervals varying from about 200 eV at the beginning of the energy range to about 5 keV at the end of the energy range, corrected for the self-shielding effect by using the relation of Eq. (5) (see also Fig.6). Above 40 keV the correction was negligible compared to the experimental errors. The errors shown in Table 2 take into account all those discussed above; these data have negligible Porter-Thomas fluctuations and are suitable for statistical model analysis. However, the 15000 effective total cross section points of Harvey et al. data should be kept in the experimental data libraries, since the high resolution of the measurements allow the search of possible intermediate structure in the data,⁶ in correlation with structure in the fission cross section.⁷ The user of the uncorrected data should note that: (a) correction for the self-shielding effect could be performed with good accuracy by using Eq. (5), with the restrictions stated above concerning the energy range for averaging the data, and (b) the corrections are not needed above 40 keV neutron energy.

Table 2. Average total cross section in the energy range 2 keV to 300 keV corrected for isotopic composition of the sample and for self-shielding effects.

Energy range eV		Average cross section b	Stat. error	Syst. error	Total error
2000.869	2181.508	20.053	0.024	0.166	0.168
2181.508	2387.761	19.815	0.024	0.159	0.161
2387.761	2624.710	19.781	0.024	0.153	0.155
2624.710	2898.763	18.629	0.023	0.143	0.144
2898.763	3218.090	18.335	0.023	0.137	0.139
3218.090	3593.243	18.540	0.023	0.135	0.137
3593.243	4038.035	18.023	0.023	0.130	0.132
4038.035	4570.833	17.900	0.023	0.128	0.130
4570.833	4791.162	17.756	0.037	0.126	0.131

Table 2 (Contd.)

Energy range eV		Average cross section b	Stat. error	Syst. error	Total error
4791.162	5027.813	16.930	0.038	0.122	0.128
5027.813	5282.442	16.708	0.038	0.121	0.127
5282.442	5556.916	16.752	0.038	0.120	0.126
5556.916	5853.351	16.924	0.037	0.121	0.126
5853.351	6174.154	17.247	0.057	0.122	0.134
6174.154	6522.072	16.618	0.037	0.119	0.125
6522.072	6900.249	16.272	0.037	0.117	0.123
6900.249	7312.298	16.104	0.037	0.116	0.122
7312.298	7762.390	16.145	0.036	0.116	0.122
7762.390	8255.354	15.929	0.037	0.115	0.121
8255.354	8796.812	16.321	0.036	0.117	0.122
8796.812	9393.342	15.905	0.036	0.115	0.120
9393.342	10052.674	15.929	0.036	0.115	0.120
10052.674	10264.043	15.818	0.065	0.114	0.132
10264.043	10482.150	15.576	0.065	0.113	0.131
10482.150	10707.283	15.119	0.065	0.112	0.129
10707.283	10939.750	15.437	0.065	0.113	0.130
10939.750	11179.868	15.660	0.064	0.114	0.130
11179.868	11427.980	15.483	0.064	0.113	0.130
11427.980	11684.445	15.253	0.065	0.112	0.130
11684.445	11949.640	15.394	0.064	0.113	0.129
11949.640	12223.969	15.218	0.064	0.112	0.129
12223.969	12507.852	15.115	0.064	0.112	0.129
12507.852	12702.639	14.968	0.079	0.111	0.136
12702.639	12902.008	14.966	0.078	0.111	0.136

Table 2 (Contd.)

Energy range eV		Average cross section b	Stat. error	Syst. error	Total error
12902.008	13106.111	14.984	0.080	0.111	0.137
13106.111	13315.096	15.161	0.078	0.112	0.136
13315.096	13529.119	15.396	0.078	0.112	0.137
13529.119	13748.344	15.204	0.078	0.112	0.136
13748.344	13972.939	14.824	0.078	0.110	0.135
13972.939	14203.086	15.065	0.078	0.111	0.136
14203.086	14438.966	14.821	0.079	0.110	0.136
14438.966	14680.770	14.987	0.077	0.111	0.135
14680.770	14928.701	14.931	0.078	0.111	0.135
14928.701	15182.963	15.038	0.077	0.111	0.135
15182.963	15443.780	14.713	0.077	0.110	0.134
15443.780	15711.375	14.762	0.077	0.110	0.134
15711.375	15985.984	14.667	0.077	0.110	0.134
15985.984	16267.858	14.737	0.077	0.110	0.134
16267.858	16557.252	14.805	0.077	0.110	0.134
16557.252	16854.439	14.911	0.080	0.111	0.136
16854.439	17159.701	14.869	0.076	0.110	0.134
17159.701	17473.328	14.684	0.076	0.110	0.134
17473.328	17795.637	14.628	0.076	0.110	0.133
17795.637	18126.941	14.567	0.076	0.109	0.133
18126.941	18467.590	14.833	0.075	0.110	0.133
18467.590	18817.930	14.560	0.075	0.109	0.133
18817.930	19178.332	14.419	0.076	0.109	0.133
19178.332	19549.193	14.458	0.075	0.109	0.132
19549.193	19930.914	14.365	0.075	0.109	0.132

Table 2 (Contd.)

Energy range eV		Average cross section b	Stat. error	Syst. error	Total error
19930.914	20125.979	14.476	0.106	0.109	0.152
20125.979	20323.926	14.364	0.106	0.109	0.152
20323.926	20524.805	14.191	0.106	0.108	0.151
20524.805	20728.678	14.191	0.106	0.108	0.151
20728.678	20935.602	14.440	0.105	0.109	0.151
20935.602	21145.641	14.736	0.104	0.110	0.151
21145.641	21358.855	13.891	0.106	0.107	0.151
21358.855	21575.314	14.293	0.104	0.108	0.150
21575.314	21795.078	13.967	0.104	0.107	0.149
21795.078	22018.219	14.571	0.102	0.109	0.149
22018.219	22244.801	14.336	0.103	0.108	0.150
22244.801	22474.902	14.634	0.103	0.110	0.150
22474.902	22708.590	14.413	0.103	0.109	0.150
22708.590	22945.943	14.464	0.103	0.109	0.150
22945.943	23187.035	14.144	0.103	0.108	0.149
23187.035	23431.945	14.159	0.103	0.108	0.149
23431.945	23680.762	13.885	0.104	0.107	0.149
23680.762	23933.561	14.126	0.103	0.108	0.149
23933.561	24190.430	13.931	0.104	0.107	0.149
24190.430	24451.453	14.101	0.103	0.108	0.149
24451.453	24716.727	13.900	0.103	0.107	0.148
24716.727	24986.340	14.362	0.101	0.109	0.148
24986.340	25260.391	14.032	0.103	0.107	0.149
25260.391	25538.975	14.447	0.109	0.109	0.154
25538.975	25822.191	14.006	0.102	0.107	0.148

Table 2 (Contd.)

Energy range eV		Average cross section b	Stat. error	Syst. error	Total error
25822.191	26110.145	13.510	0.103	0.106	0.148
26110.145	26402.943	14.116	0.101	0.108	0.148
26402.943	26700.695	13.887	0.102	0.107	0.148
26700.695	27003.516	13.970	0.102	0.107	0.148
27003.516	27311.512	14.001	0.101	0.107	0.147
27311.512	27624.805	14.172	0.101	0.108	0.148
27624.805	27943.527	13.928	0.102	0.107	0.148
27943.527	28267.795	14.169	0.101	0.108	0.148
28267.795	28597.742	13.670	0.102	0.106	0.147
28597.742	28933.496	13.479	0.103	0.106	0.147
28933.496	29275.197	14.376	0.100	0.109	0.148
29275.197	29622.992	14.001	0.103	0.107	0.149
29622.992	29977.020	13.780	0.102	0.107	0.147
29977.020	30337.434	13.902	0.105	0.107	0.150
30337.434	30704.383	13.991	0.126	0.107	0.165
30704.383	31078.031	13.863	0.103	0.107	0.148
31078.031	31458.545	13.820	0.104	0.107	0.149
31458.545	31846.090	13.923	0.105	0.107	0.150
31846.090	32240.842	13.751	0.108	0.106	0.152
32240.842	32642.971	13.349	0.114	0.105	0.155
32642.971	33052.684	14.157	0.119	0.108	0.161
33052.684	33470.148	13.438	0.133	0.105	0.170
33470.148	33895.578	13.899	0.149	0.107	0.183
33895.578	34329.172	13.998	0.177	0.107	0.207
34329.172	34771.133	14.322	0.209	0.108	0.235

Table 2 (Contd.)

Energy range eV		Average cross section b	Stat. error	Syst. error	Total error
34771.133	35221.691	13.453	0.236	0.105	0.258
35221.691	35681.063	13.461	0.228	0.105	0.251
35681.063	36149.477	13.830	0.197	0.107	0.224
36149.477	36627.176	13.504	0.178	0.106	0.207
36627.176	37114.406	13.580	0.154	0.106	0.187
37114.406	37611.430	13.364	0.141	0.105	0.176
37611.430	38118.500	13.451	0.133	0.105	0.170
38118.500	38635.898	13.169	0.124	0.104	0.162
38635.898	39163.898	13.150	0.119	0.104	0.158
39163.898	39702.797	13.537	0.114	0.106	0.155
39702.797	40252.898	13.418	0.112	0.105	0.154
40252.898	40814.512	13.367	0.110	0.105	0.152
40814.512	41387.961	13.295	0.115	0.105	0.156
41387.961	41973.586	13.586	0.116	0.106	0.157
41973.586	42571.723	13.020	0.114	0.104	0.154
42571.723	43182.742	13.393	0.109	0.105	0.151
43182.742	43807.008	13.400	0.107	0.105	0.150
43807.008	44444.906	13.303	0.105	0.105	0.148
44444.906	45096.852	13.190	0.105	0.105	0.148
45096.852	45763.234	13.051	0.104	0.104	0.147
45763.234	46444.508	13.061	0.103	0.104	0.146
46444.508	47141.102	13.223	0.101	0.105	0.145
47141.102	47853.492	13.208	0.104	0.105	0.147
47853.492	48582.152	13.070	0.100	0.104	0.144
48582.152	49327.578	13.263	0.099	0.105	0.144

Table 2 (Contd.)

Energy range eV		Average cross section b	Stat. error	Syst. error	Total error
49327.578	50090.301	13.128	0.099	0.104	0.144
50090.301	50713.285	12.919	0.111	0.104	0.152
50713.285	51347.965	12.989	0.110	0.104	0.151
51347.965	51994.633	12.925	0.110	0.104	0.151
51994.633	52653.598	13.287	0.108	0.105	0.151
52653.598	53325.172	12.767	0.109	0.103	0.150
53325.172	54009.680	13.042	0.108	0.104	0.150
54009.680	54707.445	12.881	0.108	0.104	0.150
54707.445	55418.824	13.157	0.104	0.104	0.147
55418.824	56144.172	13.343	0.093	0.105	0.140
56144.172	56883.852	12.895	0.099	0.104	0.143
56883.852	57638.250	12.883	0.101	0.104	0.145
57638.250	58407.750	13.154	0.101	0.104	0.145
58407.750	59192.766	12.835	0.102	0.103	0.145
59192.766	59993.715	12.836	0.102	0.103	0.145
59993.715	60811.031	12.748	0.103	0.103	0.146
60811.031	61645.168	12.823	0.102	0.103	0.145
61645.168	62496.586	12.795	0.103	0.103	0.146
62496.586	63365.766	12.586	0.103	0.103	0.145
63365.766	64253.207	12.762	0.103	0.103	0.146
64253.207	65159.422	12.628	0.102	0.103	0.145
65159.422	66084.945	12.594	0.102	0.103	0.145
66084.945	67030.328	12.870	0.102	0.103	0.145
67030.328	67996.148	12.799	0.100	0.103	0.144
67996.148	68982.992	12.798	0.101	0.103	0.144

Table 2 (Contd.)

Energy range eV		Average cross section b	Stat. error	Syst. error	Total error
68982.992	69991.469	12.663	0.101	0.103	0.144
69991.469	71022.234	12.439	0.102	0.102	0.144
71022.234	72075.938	12.447	0.106	0.102	0.147
72075.938	73153.266	12.614	0.100	0.103	0.143
73153.266	74254.930	12.496	0.101	0.102	0.144
74254.930	75381.672	12.551	0.101	0.102	0.144
75381.672	76534.258	12.458	0.102	0.102	0.144
76534.258	77713.484	12.367	0.109	0.102	0.149
77713.484	78920.172	12.737	0.134	0.103	0.169
78920.172	80155.188	12.254	0.112	0.102	0.151
80155.188	81419.422	12.265	0.111	0.102	0.150
81419.422	82713.805	12.389	0.116	0.102	0.154
82713.805	84039.305	12.279	0.125	0.102	0.161
84039.305	85396.922	12.697	0.134	0.103	0.169
85396.922	86787.703	12.202	0.149	0.101	0.180
86787.703	88212.750	11.691	0.156	0.100	0.185
88212.750	89673.188	12.476	0.148	0.102	0.180
89673.188	91170.195	12.136	0.147	0.101	0.178
91170.195	92705.008	12.231	0.137	0.101	0.170
92705.008	94278.906	12.299	0.122	0.102	0.159
94278.906	95893.234	12.226	0.117	0.101	0.155
95893.234	97549.375	11.734	0.118	0.100	0.155
97549.375	99248.797	12.178	0.117	0.101	0.155
99248.797	100993.031	11.965	0.115	0.101	0.153
100993.031	101882.438	11.728	0.165	0.100	0.193

Table 2 (Contd.)

Energy range eV		Average cross section b	Stat. error	Syst. error	Total error
101882.438	102783.641	12.073	0.164	0.101	0.193
102783.641	103696.867	11.920	0.164	0.100	0.192
103696.867	104622.313	11.587	0.165	0.099	0.193
104622.313	105560.203	12.170	0.159	0.101	0.189
105560.203	106510.766	11.885	0.157	0.100	0.186
106510.766	107474.219	11.999	0.153	0.101	0.183
107474.219	108450.813	12.139	0.151	0.101	0.182
108450.813	109440.781	11.418	0.151	0.099	0.181
109440.781	110444.359	12.006	0.146	0.101	0.177
110444.359	111461.828	11.899	0.146	0.100	0.177
111461.828	112493.398	11.538	0.173	0.099	0.199
112493.398	113539.359	11.590	0.149	0.099	0.179
113539.359	114599.984	11.916	0.138	0.100	0.171
114599.984	115675.539	11.424	0.141	0.099	0.172
115675.539	116766.313	11.333	0.139	0.099	0.170
116766.313	117872.578	11.772	0.149	0.100	0.179
117872.578	118994.656	11.691	0.146	0.100	0.177
118994.656	120132.828	11.556	0.168	0.099	0.195
120132.828	121287.398	11.879	0.168	0.100	0.196
121287.398	122458.703	11.800	0.142	0.100	0.174
122458.703	123647.055	11.618	0.130	0.100	0.164
123647.055	124852.797	11.408	0.130	0.099	0.163
124852.797	126076.250	11.556	0.124	0.099	0.159
126076.250	127317.781	11.730	0.119	0.100	0.155
127317.781	128577.750	11.543	0.121	0.099	0.157

Table 2 (Contd.)

Energy range eV		Average cross section b	Stat. error	Syst. error	Total error
128577.750	129856.516	11.512	0.117	0.099	0.153
129856.516	131154.438	11.559	0.116	0.099	0.153
131154.438	132471.953	11.777	0.114	0.100	0.152
132471.953	133809.406	11.664	0.113	0.100	0.151
133809.406	135167.203	11.489	0.114	0.099	0.151
135167.203	136545.781	11.327	0.117	0.099	0.153
136545.781	137945.563	11.359	0.121	0.099	0.156
137945.563	139366.984	11.525	0.123	0.099	0.158
139366.984	140810.484	11.250	0.132	0.098	0.165
140810.484	142276.531	11.736	0.132	0.100	0.166
142276.531	143765.609	11.529	0.135	0.099	0.168
143765.609	145278.172	11.165	0.138	0.098	0.169
145278.172	146814.750	11.015	0.139	0.098	0.170
146814.750	148375.813	11.093	0.135	0.098	0.167
148375.813	149961.938	11.387	0.132	0.099	0.165
149961.938	151573.609	11.222	0.132	0.098	0.165
151573.609	153211.406	10.947	0.124	0.098	0.158
153211.406	154875.922	10.864	0.122	0.097	0.156
154875.922	156567.688	10.907	0.122	0.097	0.156
156567.688	158287.344	11.472	0.130	0.099	0.163
158287.344	160035.469	11.176	0.140	0.098	0.171
160035.469	161812.734	10.885	0.124	0.097	0.158
161812.734	163619.781	11.016	0.111	0.098	0.148
163619.781	165457.250	10.700	0.106	0.097	0.144
165457.250	167325.844	10.935	0.101	0.098	0.140

Table 2 (Contd.)

Energy range eV		Average cross section b	Stat. error	Syst. error	Total error
167325.844	169226.313	11.047	0.098	0.098	0.138
169226.313	171159.313	10.998	0.095	0.098	0.136
171159.313	173125.625	10.877	0.093	0.097	0.135
173125.625	175126.031	10.807	0.089	0.097	0.132
175126.031	177161.313	10.868	0.086	0.097	0.130
177161.313	179232.281	10.682	0.084	0.097	0.128
179232.281	181339.781	10.737	0.082	0.097	0.127
181339.781	183484.688	10.620	0.080	0.097	0.125
183484.688	185667.875	10.733	0.077	0.097	0.124
185667.875	187890.266	10.754	0.075	0.097	0.123
187890.266	190152.781	10.729	0.074	0.097	0.122
190152.781	192456.438	10.625	0.072	0.097	0.120
192456.438	194802.219	10.505	0.070	0.096	0.119
194802.219	197191.141	10.389	0.069	0.096	0.118
197191.141	199624.281	10.615	0.069	0.097	0.119
199624.281	202102.750	10.629	0.072	0.097	0.121
202102.750	204627.656	10.639	0.077	0.097	0.124
204627.656	207200.203	10.439	0.072	0.096	0.120
207200.203	209821.563	10.442	0.071	0.096	0.119
209821.563	212492.969	10.485	0.067	0.096	0.117
212492.969	215215.781	10.552	0.063	0.096	0.115
215215.781	217991.219	10.389	0.061	0.096	0.114
217991.219	220820.719	10.405	0.058	0.096	0.112
220820.719	223705.672	10.215	0.058	0.095	0.112
223705.672	226647.563	10.272	0.057	0.096	0.111

Table 2 (Contd.)

Energy range eV		Average cross section b	Stat. error	Syst. error	Total error
226647.563	229647.844	10.194	0.054	0.095	0.110
229647.844	232708.109	10.068	0.053	0.095	0.109
232708.109	235829.969	10.108	0.052	0.095	0.108
235829.969	239015.078	10.148	0.051	0.095	0.108
239015.078	242265.156	10.182	0.050	0.095	0.108
242265.156	245582.000	10.182	0.049	0.095	0.107
245582.000	248967.453	9.954	0.049	0.095	0.107
248967.453	252423.391	10.102	0.049	0.095	0.107
252423.391	255951.781	9.946	0.048	0.095	0.106
255951.781	259554.703	9.924	0.051	0.095	0.108
259554.703	263234.250	9.909	0.049	0.095	0.107
263234.250	266992.625	9.951	0.048	0.095	0.106
266992.625	270832.063	9.829	0.049	0.094	0.106
270832.063	274754.906	9.791	0.051	0.094	0.107
274754.906	278763.625	9.829	0.053	0.094	0.108
278763.625	282860.750	9.724	0.057	0.094	0.110
282860.750	287048.875	9.660	0.060	0.094	0.111
287048.875	291330.719	9.730	0.062	0.094	0.113
291330.719	295709.125	9.482	0.060	0.093	0.111
295709.125	300187.000	9.534	0.060	0.094	0.111
300187.000	304767.375	9.569	0.060	0.094	0.111
304767.375	309453.375	9.520	0.061	0.094	0.112
309453.375	314248.313	9.436	0.064	0.093	0.113
314248.313	319155.625	9.483	0.072	0.093	0.118
319155.625	324178.813	9.529	0.105	0.094	0.141

Comparisons with other experimental results are shown in Figs. 2 and 3. The data of Uttley⁸ were obtained in 1970 at the Electron Linear Accelerator of Harwell. The data of Poenitz et al.⁴ were obtained in 1981 at the Argonne National Laboratory Fast Neutron Generator in the energy range above 40 keV. Comparison between Poenitz results and the present results averaged over the energy ranges of Poenitz experimental resolution is shown on Table 3. The agreement is excellent. Uttley data are 8% to 12% higher. The Uttley experiments were performed with samples of 81.2% of ²³⁵U; however, the differences could hardly be explained by errors on the corrections for the contribution of the other isotopes. Instead it is likely that the data compiled for the EXFOR⁹ file were not corrected for the isotopic contributions; that could explain differences of 5% to 10%.

Table 3. Comparison between the experimental cross section of Poenitz et al.⁴ with the present results averaged over the energy resolution of Poenitz.

Energy keV	Poenitz data		Present Data		Difference %
	barn	barn	barn	barn	
48	13.22	0.17	13.15	0.104	-0.5
63	12.77	0.21	12.82	0.103	0.4
78	12.31	0.16	12.47	0.103	1.3
92	12.08	0.16	12.15	0.101	0.6
111	11.74	0.15	11.80	0.100	0.5
137	11.38	0.15	11.43	0.099	0.5
172	10.89	0.15	10.93	0.097	0.4
195	10.54	0.10	10.66	0.096	1.1
223	10.32	0.15	10.43	0.095	1.1
244	10.15	0.12	10.06	0.095	-0.9
297	9.67	0.09	9.67	0.094	0.0

The total cross sections in ENDF/B-VI are compared to the present data in Fig. 4 in the energy range 2 keV to 300 keV. The agreement in the energy range above 40 keV is particularly good due to the fact that the ENDF/B-VI evaluation was based on Poenitz data. Below 30 keV, ENDF/B-VI is on average 1.7% larger. In this energy range Weston¹⁰ used an early version of the statistical model code FITACS¹¹ to fit the standard fission cross section¹² along with recent measurements of α (ratio of the capture to the fission), and used the current values of the neutron strength functions and effective scattering radius for the calculation of the total cross section. A new evaluation should be performed in order to obtain agreement better than 1.7% with the present data. The basis for a new evaluation in the unresolved energy range is presented in the next section from a statistical analysis of the experimental data.

Note in Figs. 2, 3, and 4, that the data were averaged by using an energy mesh different from that of Table 2, to allow better comparison with the other experimental data and ENDF/B-VI.

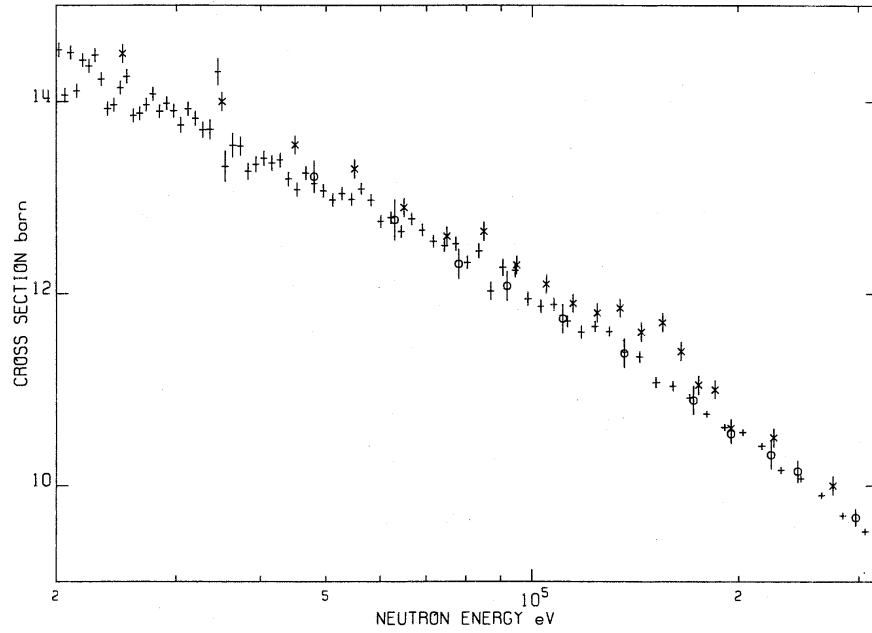


Figure 2. Average total cross section in the energy range from 20 keV to 300 keV: present results (+), Uttley⁸ data (x) and Poenitz⁴ data (o).

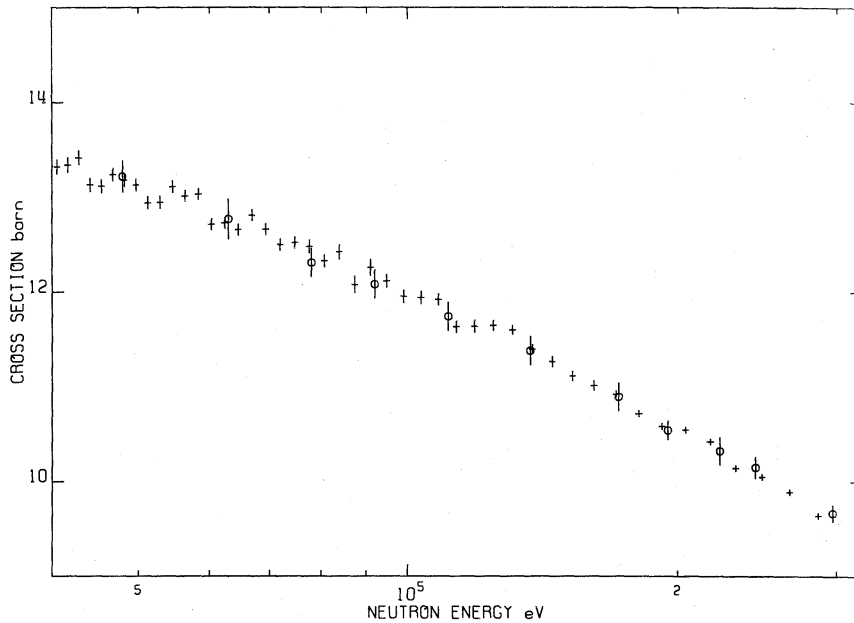


Figure 3. Average total cross section in the energy range 40 keV to 300 keV: present results (+) and Poenitz⁴ data (o).

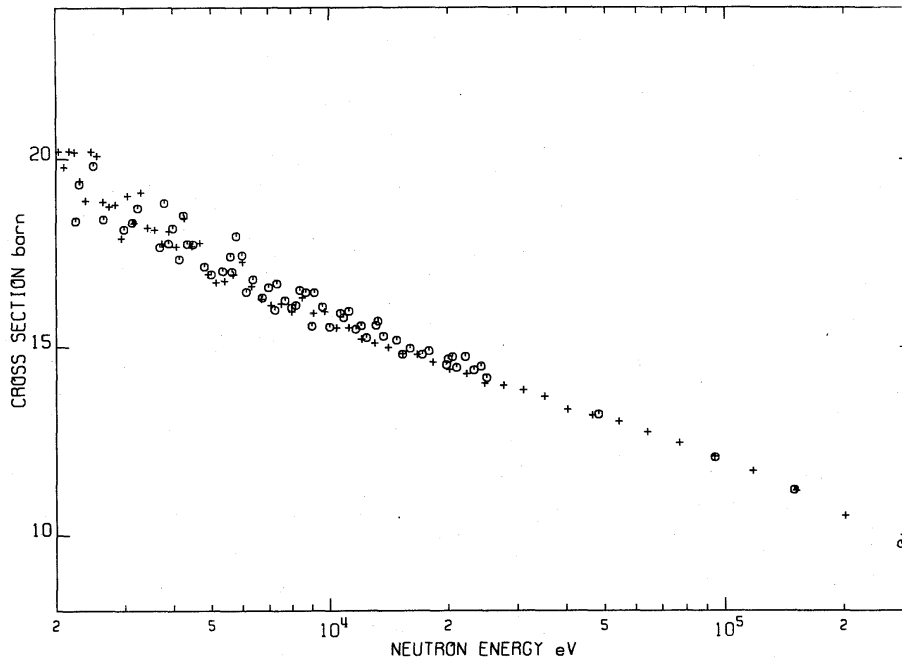


Figure 4. Average total cross section in the energy range 2 keV and 300 keV: present results (+) and ENDF/B-VI data (o).

3. STATISTICAL MODEL ANALYSIS OF THE EXPERIMENTAL DATA

In the present work, selected experimental fission cross sections and α data were analyzed along with the experimental total cross section. The fission experimental data base for ^{235}U contains a very large amount of data which were all considered by the ENDF/B-VI standard evaluation working group.¹² The current ENDF/B-VI fission cross section was obtained by renormalizing the ENDF/B-V data to the standard values in the energy range 2.25 keV to 100 keV, preserving the main structures of the experimental cross section. The ENDF/B-VI capture cross section was calculated by multiplying the fission cross section by the values of α obtained by Weston from an eye-guided fit of the experimental data of Corvi et al.¹³ and of Muradyan et al.¹⁴ Weston did not take into account the highest values of α , which are mainly the results of the high resolution measurements of Beer et al.¹⁵ and the RPI data of de Saussure et al.¹⁶ at about 10% above Corvi data in the energy range 20 keV to 100 keV.

The present SAMMY/FITACS analysis is a statistical model fit of the new average total cross section and of selected experimental fission and α data, including Beer and de Saussure data, with a search for a possible renormalization of the fission and capture data.

3.1 THE SAMMY/FITACS STATISTICAL MODEL CODE

The statistical model code FITACS of F.H. Froehner was incorporated into SAMMY by N.M. Larson. FITACS uses the Hauser-Feshbach theory for the calculation of the average total and partial cross sections. The input parameters for the calculation of the theoretical data are mainly the neutron strength functions, the average level density and the average partial widths at low energy, the distant-level parameters, the energy, spin and parity of the low-lying levels of the target nucleus, and the fission barrier parameters. The energy dependence of the average resonance parameters is obtained from the Bethe formula for the level density, from the Hill-Wheeler fission barrier penetration for the fission widths, and from the giant dipole model resonance for the capture widths. The Moldauer method is used for the calculation of the width fluctuation corrections. A consistent fit to the input experimental total and partial cross sections is obtained by solving the Bayes equations relative to the variable parameters. The a priori values of the average resonance parameters could be available from the statistical analysis of the resonance parameters in the resolved resonance region or from optical model calculations.

The input experimental cross sections are the averaged experimental data with their statistical errors. The resonance structures of the experimental data are generally washed out by the experimental resolution and the Doppler broadening in the high-energy part of the data. In the lower-energy region, just above the upper limit of the resolved range, the fluctuations due to the resonances are still present; further averaging could be needed before using the data as input for a statistical model fit. Intermediate structures, particularly those due to a double-humped fission barrier, could also be present in some experimental fission data; these structures could not be described by the statistical model of FITACS. The intermediate structures are more likely present in the ^{235}U fission data.^{3,7,15,17} The high-resolution measurements of α by Beer et al.¹⁵ showed structures correlated with structures in Perez et al.¹⁸ fission data. The parameters of the intermediate structures in the fission data have the statistical properties of the Class-II resonances (levels of the second well of a double humped fission barrier) with an average spacing of about 500 eV^{15} which is 1000 times larger than the average spacing of the Class-I resonances. However, the amplitude of the ^{235}U fission structures is quite small compared to the average fission cross section and the statistical analysis should be a reasonable approximation for the fit of the data, but the statistical errors on the input data should be increased to include the possible remaining non-statistical fluctuations of the average cross section.

3.2 THE SAMMY/FITACS FIT OF THE AVERAGE CROSS SECTION

The statistical model fit of the average total cross section in the unresolved energy range is straightforward, involving a small number of parameters which are the strength functions S_l relative to the different angular momentum l , and the nuclear radius parameters. Prior to the fit, the strength functions could be obtained from the neutron transmission coefficients calculated by the optical model, when they are not available from statistical analysis of resonance parameters. The contribution of the $l = 0, 1, 2,$ and 3 angular momentum to the total cross section is about 69%, 30%, 2.5% and 0.4%, respectively, at 300 keV neutron energy. Therefore the fit to the total cross section in the energy range up to 300 keV should provide accurate values for the $l = 0$ and $l = 1$ parameters, but poor accuracy for the $l = 2$ and $l = 3$ parameters.

The input parameters for the SAMMY/FITACS calculations are given in Table 4. The $l = 0$ parameters are those obtained from the statistical study of the resonance parameters in the energy range 0 eV to 2250 eV in Ref. 3. The value -0.145 of the s-wave distant level parameter R^∞ was obtained from the effective scattering radius $R' = 9.602\text{ fm}$ of Ref. 3 by the relation

$$R' = R(1 - R^\infty) \text{ fm},$$

with the nuclear radius,

$$R = 1.23A^{1/3} + 0.8 \text{ fm}$$

used as default value in SAMMY/FITACS. Some parameters for $l = 1$ and $l = 2$ angular momentum were taken from Ref. 8. The energies of the ^{235}U low lying levels were taken from Nuclear Data Sheets¹⁹, and the fission barrier parameters from Bjornholm and Lynn.²⁰

Table 4. The parameters used as input in the SAMMY/FITACS calculations

Input Parameters of s-wave Resonances	
Average Level Spacing	$D = 0.446 \pm 0.031 \text{ eV}$
Neutron Strength Function	$S_0 = (1.049 \pm 0.024)10^{-4}$
Capture Width	$\Gamma_\gamma = 38.14 \pm 1.70 \text{ meV}$
Effective Scattering Radius	$R' = 9.602 \pm 0.050 \text{ fm}$
Distant Level Parameter	$R^\infty = -0.155 \pm 0.006$
3 ⁻ channel Fission Width	$\Gamma_f = 213.0 \pm 20 \text{ meV}$
4 ⁻ channel Fission Width	$\Gamma_f = 146.5 \pm 15 \text{ meV}$
Input Parameters of p-wave Resonances	
Neutron Strength Function	$S_1 = (1.76 \pm 0.25)10^{-4}$
Distant Level Parameter	$R^\infty = 0.02 \pm 0.03$
Capture Width	$\Gamma_\gamma = 38.14 \pm 10.00 \text{ meV}$
Fission Widths (2+ to 5+ channels)	$\Gamma_f = 200 \pm 100 \text{ meV}$
Input Parameters of d-wave Resonances	
Neutron Strength Function	$S_2 = (0.60 \pm 0.50)10^{-4}$
Distant Level Parameter	$R^\infty = -0.100 \pm 0.050$
Capture Width	$\Gamma_\gamma = 38.14^*$
Fission Widths (other than 3 ⁻ and 4 ⁻)	$\Gamma_f = 200 \pm 100 \text{ meV}$

*The average capture width of the d-wave resonances is assumed to be the same as for s-waves in SAMMY/FITACS calculation.

In the neutron energy range of interest, one assumed that the fission induced by the s-wave neutrons proceeds through two 3^- and two 4^- open fission channels, according to the statistical properties of the fission widths in the resolved resonance region. The fission induced by the p-wave neutrons proceeds through the fission channels of spin and parity 2^+ , 3^+ , 4^+ and 5^+ for which there is no information from the resolved resonance parameters. Candidates for these fission channels could be found in the $K = 0^+$ rotational band of the ground state and in other $K = 0^+$ or $K = 2^+$ rotational bands. The corresponding fission width values at low energy should be of the same order of magnitude as those of the s-wave fission channels. The height of the lowest 3^- fission barrier was placed at 0.9 MeV below the ^{236}U neutron binding energy and the others were positioned according to the ^{236}U level scheme found in Nuclear Data Sheets,²¹ although the level scheme of the ^{236}U nucleus highly deformed at the fission barrier could be very different from that at its stable deformation. Actually, all of the fission channels considered are open channels; therefore the values of the cross section below 200 keV neutron energy will not be very sensitive to the exact energy position of the fission barriers. In the neutron energy range below 200 keV, the only important contribution to the fission comes from the s- and p- wave resonances; therefore the fission parameters are needed especially for the 3^- , 4^- , 2^+ , 3^+ , 4^+ and 5^+ fission channels. The small contribution of the d-wave neutrons could be calculated by the parameters of the 3^- and 4^- channels. The average fission widths at thermal energy are the adjustable fission parameters in SAMMY/FITACS; the fission barrier parameters are needed only for the dependence in energy of the average fission widths. The parameters for the description of the structures, if any, due to double-humped fission barriers, are not considered in SAMMY/FITACS; the corresponding small fluctuations in the average experimental cross section will be interpreted as statistical fluctuations in FITACS calculations.

The following experimental fission cross sections were considered in the experimental data base:

1. Blons²² data in the energy range 2 keV to 30 keV (Saclay linac, 1972).
2. Migneco et al.²³ data in the energy range 2 keV to 200 keV (GELINA, 1975).
3. Wagemans et al.²⁴ data in the energy range 2 keV to 30 keV (GELINA, 1976).
4. Perez et al.²⁵ data in the energy range 2 keV to 100 keV (ORELA, 1973).
5. Weston et al.²⁶ data in the energy range 2 keV to 200 keV (ORELA, 1984).

All these data were the results of high-resolution time-of-flight measurements analyzed at low energy for the determination of the resonance parameters. In general, the normalization of the fission cross sections were performed by the authors relative to the available standard data at thermal energy, directly or indirectly, with an accuracy of about 2%. However, due to unknown experimental effects, the data are not consistent in the energy range above 2 keV, showing discrepancies as large as 6% of the average cross section. One assumes in the present work that a consistent renormalization of the data in the energy range 2 keV to 200 keV could be obtained by the current version of SAMMY/FITACS from a Bayesian search of a renormalization coefficient. Prior to the SAMMY analysis, the experimental data were averaged using a common energy mesh of 140 points, in order to attenuate the non-statistical fluctuations of the cross sections.

The following measurements of the capture-to-fission ratio, α , were also considered:

1. Weston et al.²⁷ data in the energy range 1 keV to 200 keV(RPI, 1964).
2. de Saussure et al.¹⁶ data in the energy range 17 keV to 200 keV(RPI, 1965).
3. Beer et al.¹⁵ data in the energy range 10 keV to 300 keV(Karlsruhe, 1979).
4. Muradyan et al.¹⁴ data in the energy range 2 keV to 50 keV(Kurchatov, 1977).
5. Corvi et al.¹³ data in the energy range 2 keV to 80 keV(GELINA, 1982).

6. Perez et al.²⁸ data in the energy range 1 keV to 10 keV(ORELA,1973).

The experimental capture-to-fission ratio is plotted in Fig. 5 in the energy range 2 keV to 200 keV. The spread of the experimental data is important and not compatible with the experimental errors. There is a remarkable amount of structures in the data; some of these structures could be due to the intermediate structure in the fission cross sections.¹⁵ The Weston evaluation for ENDF/B-VI shows the structure in the energy range 5 keV to 10 keV and a smooth behavior at higher energy. The shape of the solid line was obtained, in the present work, from an eye-guided fit of the experimental values, reproducing the structures observed in Beer data and in de Saussure data, at about 12% above the ENDF/B-VI evaluation. Since the current version of SAMMY/FITACS could not directly fit the experimental values of α , an average capture cross section file CAP was created by multiplying the average fission cross sections of Weston et al.²⁶ by the values of α corresponding to the solid line of Fig. 5. The same procedure was also used by Weston for the ENDF/B-VI evaluation.

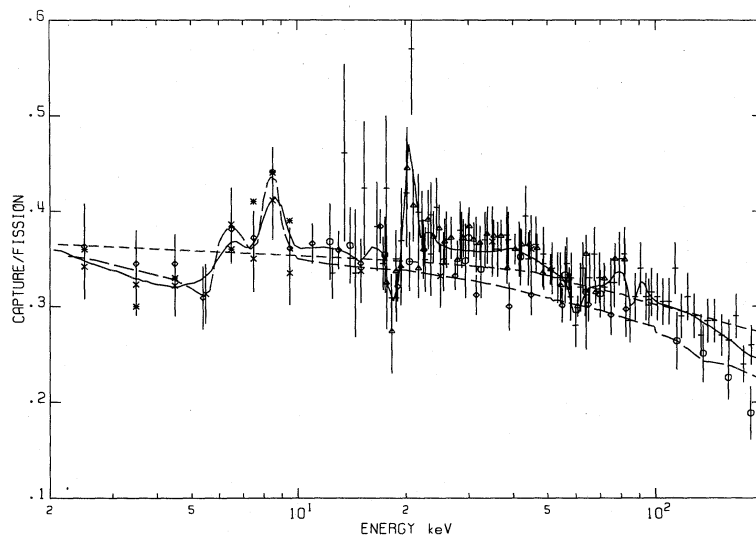


Figure 5. Experimental and calculated α values. The solid line represents an eye-guided fit of the experimental data. The short-dashed line represents the capture to fission ratio calculated at the output of the SAMMY/FITACS fit. The long-dashed line represents the values calculated from the ENDF/B-VI fission and capture cross sections.

Experimental data: Δ de Saussure et al.¹⁶
 \diamond Corvi¹³
 \circ Weston et al.²⁷
 \times Muradyan et al.¹⁴
 $+$ Beer et al.¹⁵
 $*$ Perez et al.²⁸

Finally, the experimental data base used as input in SAMMY/FITACS included the average total cross sections obtained from transmission measurements as explained in the first part of this report in the energy range up to 200 keV, the average total cross section of Poenitz et al. in the energy range 50 keV to 200 keV,

the five sets of average fission cross sections as described above, and the average capture cross section file CAP in the energy range 2 keV to 200 keV. The five sets of fission cross sections were not renormalized to a common standard prior to the SAMMY/FITACS calculation; a consistent renormalization of each set should be obtained by the Bayesian fitting procedure. Similar procedure was also applied to the capture cross section file CAP.

The parameters obtained from the fit of the experimental data base are shown in Table 5. The s-wave strength function, $(0.945 \pm 0.009)10^{-4}$, is 6% larger than the value of $(0.88 \pm 0.09)10^{-4}$ obtained from the resonance parameters in the well resolved energy range 0 eV to 110 eV, and 10% smaller than the value of $(1.049 \pm 0.024)10^{-4}$ observed in the 0 eV to 2250 eV energy range in Ref. 3 (mainly a pseudo-resonance analysis). The p-wave strength function, $(1.695 \pm 0.034)10^{-4}$, agrees with the values of Uttley; but the d-wave strength function, $(1.048 \pm 0.243)10^{-4}$, is much larger; note the accuracy of 23%, which is much better than the accuracy of 83% given by Uttley. The s-wave effective scattering radius 9.640 fm is very close to the value of 9.602 fm obtained in the resolved resonance region. The s-wave average capture width, 37.06 ± 1.50 meV, is 3% smaller than the input value 38.14 ± 1.70 meV. An interesting result is the value of 26.80 ± 1.76 meV obtained for the p-wave average capture width. The total average fission widths of the 3^- and 4^- channels, 247.3 ± 17.2 meV and 183.3 ± 10.3 meV respectively, are significantly larger than those obtained in the resolved resonance region; this result could be expected since a possible intermediate structure effect in the fission channels could modify the statistical behavior of the fission widths in the resolved resonance region. The average fission widths, 180 meV to 250 meV, obtained for the other fission channels, are consistent with the input value of 200 ± 100 meV.

The experimental data are compared with the calculated data in Figs. 6, 7, and 8. The renormalization coefficients obtained from the Bayesian simultaneous fit are given in Table 6. The calculated fission and capture cross sections are compared to ENDF/B-VI in Fig. 9. ENDF/B-VI fission cross section is about 1% higher on average in the energy range 2 keV to 20 keV and about 2% lower in the energy range 20 keV to 100 keV. In the energy range 2 keV to 10 keV, ENDF/B-VI capture cross sections agree with the calculated data within 1% on average and is smaller by about 12% over the energy range 10 keV to 200 keV. In addition to the improved accuracy on the experimental total cross section, the difference between ENDF/B-VI evaluation and the present analysis is mainly due to the consideration of larger experimental value of α in the energy range above 10 keV, as shown in Fig. 5. Note that the total inelastic scattering cross section calculated by SAMMY/FITACS decreases by about 20% at 200 keV when compared to ENDF/B-VI.

Table 5. Parameters obtained from the SAMMY/FITACS fit of the experimental cross section in the energy range 2 keV to 200 keV.

Angular Momentum	$l = 0$		$l = 1$		$l = 2$	
Neutron Strength Function $10^4 S_l$	0.945 ± 0.009		1.695 ± 0.034		1.048 ± 0.243	
Average Capture Width meV	37.06 ± 1.49		26.80 ± 1.76			
Distant Level Parameter R^*	-0.149 ± 0.002		0.124 ± 0.017		-0.048 ± 0.050	
Effective Scattering Radius R' fm	9.640 ± 0.017		7.182 ± 0.298		8.757 ± 0.334	
Fission Channel	3^-	4^-	2^+	3^+	4^+	5^+
Fission Width meV	247 ± 17	183 ± 10	203 ± 20	189 ± 18	217 ± 16	204 ± 19

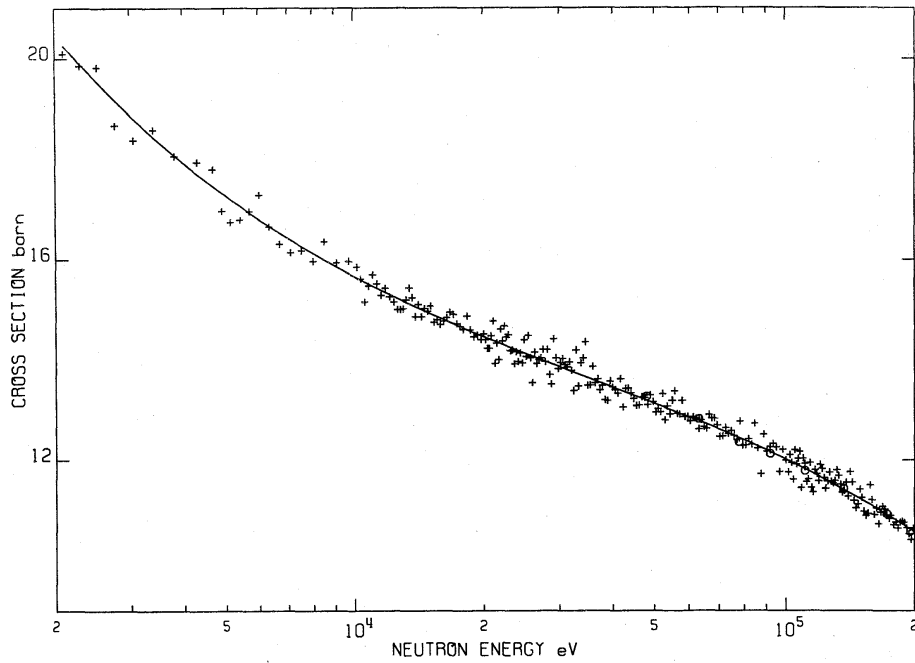


Figure 6. Average total cross sections in the energy range 2 keV to 200 keV: present results (+) and Poenitz results (o). The solid lines represent the results of the SAMMY/FITACS fit.

Table 6. The renormalization coefficients as obtained from the SAMMY/FITACS fit of the experimental data.

Experimental data	Input	Ouput
Present total	1.000 ± 0.005	0.9978 ± 0.0026
Poenitz et al. Total ⁴	1.000 ± 0.005	0.9965 ± 0.0031
Blons Fission ²²	1.000 ± 0.030	1.0082 ± 0.0137
Migneco et al. Fission ²³	1.000 ± 0.030	0.9887 ± 0.0121
Wagemans et al. Fission ²⁴	1.000 ± 0.030	1.0300 ± 0.0141
Weston et al. Fission ²⁷	1.000 ± 0.030	0.9591 ± 0.0115
Perez et al. Fission ²⁸	1.000 ± 0.030	1.0081 ± 0.0127
CAP file	1.000 ± 0.030	0.9655 ± 0.0236

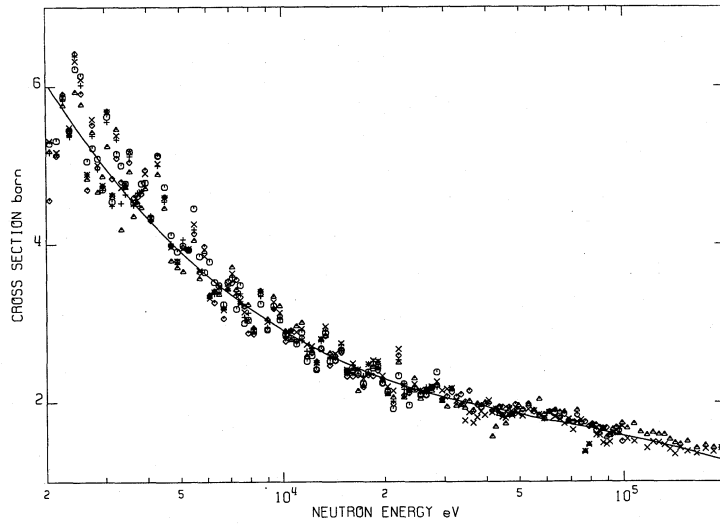


Figure 7. Average fission cross sections in the energy range 2 keV to 200 keV. The solid lines represent the results of the SAMMY/FITACS fit.

Experimental data: ○ Blons²²
 △ Migneco et al.²³
 + Wagemans et al.²⁴
 × Weston et al.²⁶
 ◇ Perez et al.²⁸

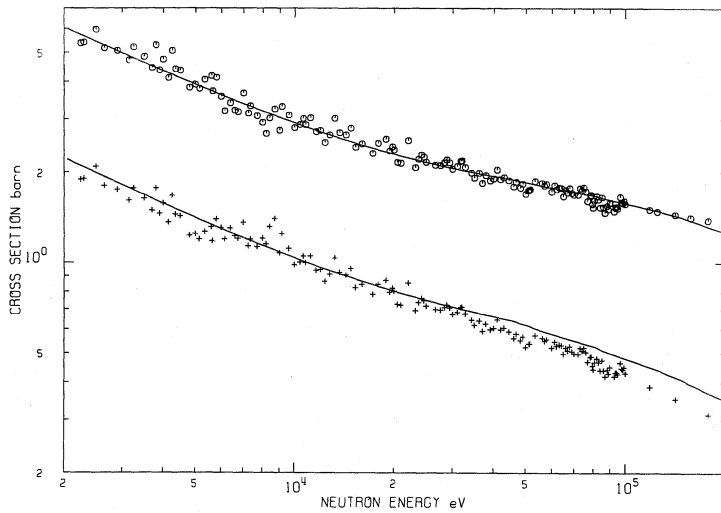


Figure 8. ENDF/B-VI fission (circles) and capture cross sections (crosses) compared to the results of the SAMMY/FITACS fit (solid line).

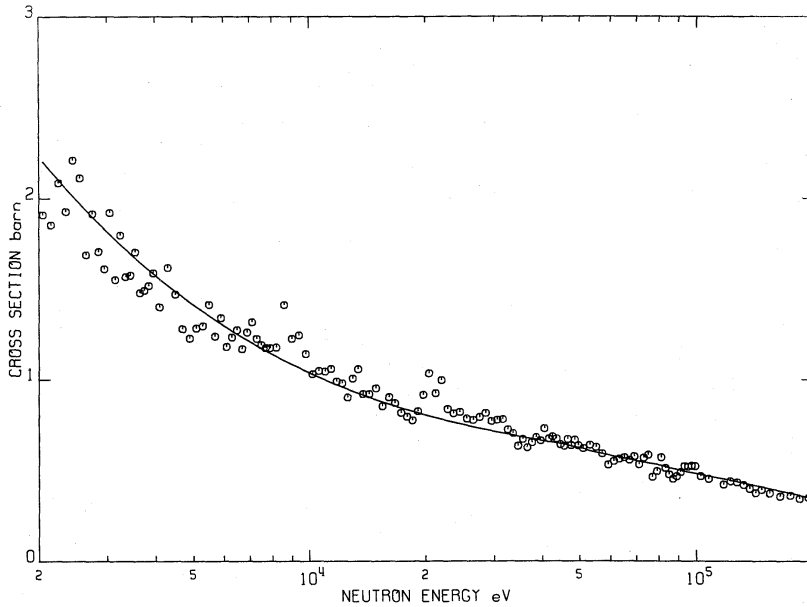


Figure 9. Average capture cross section. The solid lines represent the results of the SAMMY/FITACS fit. The circles represent the cross sections calculated by multiplying Weston fission data by the evaluated values of α . The structures are the results of the structures in Weston fission data and in the evaluated α data (the solid line in Fig.5).

4. CONCLUSION

The analysis of the high-resolution transmission data of Harvey et al. allowed the determination of the total cross section in the energy range 2 keV to 300 keV. The results meet the need of accurate data in the unresolved energy range. The data were corrected for the contribution of the other isotopes and for the self-shielding effect. The accuracy achieved is 0.8% at 2 keV and 1.5% at 300 keV. Excellent agreement was obtained with the results of Poenitz et al. in the energy range 40 keV to 300 keV. Between 2 keV and 25 keV, ENDF/B-VI data are 1.7% higher. A statistical model analysis of the data was performed along with selected average experimental fission cross sections and α data in the energy range 2 keV to 200 keV, with the newly implemented SAMMY/FITACS code. The results of the analysis show a fairly good agreement between the average resonance parameters obtained from the Reich-Moore analysis of the resolved energy range and those obtained from the statistical model analysis of the unresolved energy range. It has also been shown that ENDF/B-VI capture cross section could be too small by more than 10% in the energy range 10 keV to 200 keV. The ENDF/B-VI cross sections should be reevaluated in the unresolved-resonance region. This reevaluation should take into account the accurate experimental total cross section obtained in the present work and a careful reexamination of experimental α data in the energy range 10 keV to 200 keV.

REFERENCES

1. J. A. Harvey, N. W. Hill, F. G. Perey, G. L. Tweed, and L. C. Leal, *Proc. Int. Conf. On Nuclear Data for Science and Technology*, Mito, Japan (May 30-June 3, 1988).
2. N.M. Larson, "Updated Users' Guide for SAMMY: Multilevel R-Matrix Fits to Neutron Data Using Bayes' Equations," ORNL/TM-9179/R4 (December 1998). See also ORNL/TM-9179/R5, to be published in 2000.
3. L. C. Leal, H. Derrien, N. M. Larson, and R. Q. Wright, *Nucl. Sci. Eng.* **131**, 230 (1999).
4. W. P. Poenitz, J. F. Whalen, and A. B. Smith, *Nucl. Sci. Eng.* **78**, 333 (1981).
5. H. Derrien, *J. Nucl. Sci. Tech.* **29**(8), 794 (1992).
6. K. H. Boekhoff, A. Dufrasne, G. Rhor, and H. Weigmann, *Journal of Nuclear Energy* **26**, 91 (1972).
7. M. G. Cao, E. Migneco, and J. P. Theobald, *Phys. Lett.* **27B**, 409 (1968).
8. C.A. Uttley, *Nuclear Data for Reactors Conf.*, Vol.1, page 165, Paris (1966).
9. "EXFOR, EXchange FORmat of the Data Compilation Centers," Brookhaven National Laboratory, <http://www.dne.bnl.gov/~burrows/usnrnd/nndc.html> (July 1996).
10. L. W. Weston, "ENDF/B-VI Summary Documentation", ENDF-201, compiled and edited by P. F. Rose, Brookhaven National Laboratory, October 1991.
11. F. H. Froehner, *Nucl. Sci. Eng.* **103**, 119 (1989).
12. A. Carlson, W. P. Poenitz, G. M. Hale, R. W. Peele, D. C. Dodder, C. Y. Fu, and W. Manhart, *The ENDF/B-VI Neutron Cross Section Measurements Standards*, NISTIR-5177, National Institute of Standards and Technology, Gaithersburg, MD (May 1993).
13. F. Corvi, ANL-83-4 (1982).
14. G. V. Muradyan, Yu. G. Shepkin, Yu. V. Adamchuk and M. A. Voskanian, *Nuclear Cross Section for Technology*, Knoxville (1979).
15. H. Beer and F. Kappeler, *Phys. Rev. C*, **20**(1), 201 (1979).
16. G. de Saussure, L. W. Weston, R. Gwin, J. E. Russell, and R. W. Hockenbury, *Nucl. Sci. Eng.* **23**, 45 (1965).
17. M. S. Moore, J. D. Moses, J. A. Keyworth, J. W. T. Dabbs and N. W. Hill, *Phys. Rev. C*, **18**(3), 1328(1978).
18. R. B. Perez, G. de Saussure, and M. S. Moore, *Physics and Chemistry of Fission* (IAEA, Vienna, 1969), p.287.
19. "Nuclear Data Sheets," **36**, 3 (1982).
20. S. Bjornholm and J. E. Lynn, *Rev. Mod. Phys.*, **52**, 4, 275(1980).
21. "Nuclear Data Sheets," **40**, 1 (1983).
22. J. Blons, *Nucl. Sci. Eng.*, **51**, 130 (1973).
23. E. Migneco, P. Bonsignore, G. Lanzano, J. A. Wartena, and H. Weigmann, in *Proceedings of the Conference on Nuclear Cross Sections and Technology*, Washington, D. C., 1975, (National Bureau of Standards Special Publication No 425, 1075), Vol. II, p. 607.
24. C. Wagemans, and A. J. Deruyter, *Ann. Nucl. En.* **3**, 437 (1976).
25. R. B. Perez, G. de Saussure, E. G. Silver, R. W. Ingle, and H. Weaver, *Nucl. Sci. Eng.* **55**, 203 (1974).
26. L. W. Weston, and J. H. Todd, *Nucl. Sci. Eng.* **88**, 567 (1984).
27. L. W. Weston, G. de Saussure, R. G. Gwin, *Nucl. Sci. Eng.* **20**, 80 (1964).
28. R. B. Perez, G. De Saussure, E. G. Silver, R.W. Ingle, and H. Weaver, *Nucl. Sci. Eng.* **52**, 46 (1973).

INTERNAL DISTRIBUTION

- | | | | |
|------|-----------------|--------|---------------------------|
| 1. | B. L. Broadhead | 17. | L. C. Leal |
| 2-6. | H. Derrien | 18. | C. V. Parks |
| 7. | C. Y. Fu | 19. | R. W. Roussin |
| 8. | N. M. Greene | 20. | R. O. Sayer |
| 9. | K. Guber | 21. | M. S. Smith |
| 10. | J. A. Harvey | 22. | T. Valentine |
| 11. | C. M. Hopper | 23. | R. M. Westfall |
| 12. | D. T. Ingersoll | 24. | J. E. White |
| 13. | P. E. Koehler | 25. | R. Q. Wright |
| 14. | M. A. Kuliasha | 26. | RSICC |
| 15. | D. C. Larson | 27. | Laboratory Records |
| 16. | N. M. Larson | 28-29. | Laboratory Records (OSTI) |

EXTERNAL DISTRIBUTION

30. H. Beer, Forschungszentrum Karlsruhe, IK, BAV 425, Postfach 3640, D-76021 Karlsruhe, Germany
31. P. Blaise, DER/SPRC/LEPH, Batiment 230, Centre d'Etudes de CADARACHE, 13108 Saint Paul-lez-Durance, France
32. R. Block, Rensselaer Polytechnic Institute, Troy, NY 12180-3590
33. O. Bouland, DER/SPRC/LEPH, Batiment 230, Centre d'Etudes de CADARACHE, 13108 Saint Paul-lez-Durance, France
34. D. Cabrilla, U.S. Department of Energy, NE-40 , 19901 Germantown Road, Germantown, MD 20874-1290
35. D. E. Carlson, Reactor and Plant System Branch, Division of System Research, Office of Nuclear Regulatory Research, U. S. Nuclear Regulatory Commission, MS T- 10 G6, RM T- 10, 17, Washington, DC 20555-0001
36. R. L. Dintaman, U.S. Department of Energy, DP-13, Washington, DC 20585
37. C. Dunford, Bldg 197D, National Nuclear Data Center, Brookhaven National Laboratory, Upton, NY 11973
38. J. R. Felty, U.S. Department of Energy, DP-31 1, Washington DC 20585
39. P. Finck, Argonne National Laboratory, Reactor Analysis Division, Bldg 208, Argonne, IL 60439
40. E. Fort, DER/SPRC/LEPH, Batiment 230, Centre d'Etudes de CADARACHE, 13108 Saint Paul-lez-Durance, France
41. C. M. Frankle, NIS-6, MS J562, Los Alamos National Laboratory, Los Alamos, NM 87545
42. F. Froehner, Kernforschungszentrum Karlsruhe, Institut f. Neutronenphysik und Reackorttechnik, Postfach 336 40, D-76021 Karlsruhe, Germany
43. W. Furman, Frank Laboratory of Neutron Physics, JINR, Dubna, Russia
44. S. Ganesan, Head, Nuclear Data Section, Indira Gandhi Centra for Atomic Research, Kalpakkam 603 102, Tamilnadu, India
45. F. Gunsing, Centre D'Etudes De Saclay, F-Saclay - 91191 GIF-SUR-YVETTE Cedex, France
46. G. M. Hale, T-2, MS B243, Los Alamos National Laboratory, Los Alamos, NM 87545

47. A. Hasagawa, Nuclear Data Center, Japan Atomic Energy Research Institute, Tokai-mura, Naka-gun, Ibaraki-ken 319-11, Japan
48. R. N. Hwang, Argonne National Laboratory, Reactor Analysis Division, Bldg 208, Argonne, IL 60439
49. R. P. Jacqmin, DER/SPRC/LEPH, Batiment 230, Centre d'Etudes de CADARACHE, 13108 Saint Paul-lez-Durance, France
50. N. Janeva, Bulgarian Academy of Sciences, 72, Boul, Tzarigradsko shosse, Sofia 1784, Bulgaria
51. F. Kappeler, Forschungszentrum Karlsruhe, IK, BAV 425, Postfach 3640, D-76021 Karlsruhe, Germany
52. L. Lambros, 08 E23, U.S. Nuclear Regulatory Commission, 11555 Rockville Pike, Rockville, MD 20852-2746
53. R. Little, X-TM, MS B226, Los Alamos National Laboratory, Los Alamos, NM 87545
54. C. Lubitz, Knolls Atomic Power Laboratory, P. O. Box 1072, Schenectady, NY 12301
55. R. E. MacFarlane, T-2, MS B243, Los Alamos National Laboratory, Los Alamos, NM 87545
56. C. Mounier, CEN Saclay, DMT/SERMA/LENR, 91191 Gif Sur Yvette Cedex, France
57. D. Muir, IAEA Nuclear Data Section, Wagramerstr. 5, P. O. Box 100, A- 1400 Wien, Austria
58. C. W. Nilson, Office of Nuclear Regulatory Research, U.S. Nuclear Regulatory Commission, Mail Stop TWIN 9-F-33, Washington, DC 20555
59. C. Nordborg, OECDNEA, Le Seine St-Germain 12, Boulevard Iles, 92130 Issy-les-Moulineaux, France
60. C. Raepsaet, CEN Saclay, DMT/SERMA/LEPP, 91191 Gif Sur Yvette Cedex, France
61. M. Salvatores, DRN/P, Batiment 707, C. E. CADARACHE, 13108 Saint Paul-lez-Durance, France
62. E. Sartori, OECDNEA, Le Seine St-Germain 12, Boulevard Iles, 92130 Issy-les-Moulineaux, France
63. O. A. Shcherbakov, Petersburg Nuclear Physics Institute, 18 8 3 5 0 Gatchina, Leningrad District, Russia
64. R. Shelley, Central Bureau for Nuclear Measurements, Steenweg op Retie, 2240 Geel, Belgium
65. K. Shibata, Nuclear Data Center, Japan Atomic Energy Research Institute, Tokai-mura, Naka-gun, Ibaraki-ken 319-11, Japan
66. A. B. Smith, TD 362 D216, Argonne National Laboratory, Argonne, IL 60544
67. D. L. Smith, TD-360-L106, Argonne National Laboratory, Argonne, IL 60544
68. H. Takano, Nuclear Data Center, Japan Atomic Energy Research Institute, Tokai-mura, Ibaraki-ken 319-11, Japan
69. C. Wagemans, Central Bureau for Nuclear Measurements, Steenweg op Retie, 2240 Geel, Belgium
70. H. Weigmann, Central Bureau for Nuclear Measurements, Steenweg op Retie, 2240 Geel, Belgium
71. C. Werner, Renssalaer Polytechnic Institute, Troy, NY 12180-3590
72. R. White, Lawrence Livermore National Laboratory, P. O. Box 808, Livermore, CA 94550
73. M. Williams, Nuclear Science Center, Louisiana State University, Baton Rouge, LA 70803
74. Phillip G. Young, Los Alamos National Laboratory, MS B243 T-16 Los Alamos, New Mexico 87545